Xing Chen
Coll Intelligent Mfg Engn.
Chongqing Univ Arts & Sci, Yongchuan
China

Shun Zhou
Coll Intelligent Mfg Engn,
Chongqing Univ Arts & Sci, Yongchuan
China

Xinyong Li
Inner Mongoliar
Inner Mongolia First Machinery Grp Co Ltd
Baotou
China

Tengyuan Li
Inner Mongoliar
Inner Mongolia First Machinery Grp Co Ltd
Baotou
China

Fubing Zhang
Coll Intelligent Mfg Engn,
Chongqing Univ Arts & Sci, Yongchuan
China

Xiao Peng
Coll Intelligent Mfg Engn,
Chongqing Univ Arts & Sci, Yongchuan
China

Hongting Song
Coll Intelligent Mfg Engn,
Chongqing Univ Arts & Sci, Yongchuan
China

A Combined Weighting-Based Multi-Objective Topology Optimization Framework: Methodology and Application to a Hovercraft Gearbox

To address the limitations of single weighting schemes and static-dynamic performance trade-offs in gearbox topology optimization, this paper proposes a universal multi-objective framework integrating game-theory combined weighting (AHP-entropy method) and compromise programming. Applied to a hovercraft reducer housing, the method establishes a joint weight allocation model coupling compliance and the first four natural frequencies. Topology optimization via the SIMP variable density method and secondary CAD reconstruction demonstrate superior convergence robustness compared to single weighting strategies. The optimized housing achieves a 4.2% mass reduction and a 60.0% decrease in maximum stress, while raising the 4th-order natural frequency to successfully avoid the 200 Hz excitation band. This generalized methodology provides standard guidance for multi-performance collaborative optimization of transmission housings.

Keywords: *Multi-objective topology optimization; Combined weighting method; Compromise programming method;Hovercraft reducer*

1. INTRODUCTION

Lightweight design, high structural strength and low vibration are core requirements for transmission housing development. Multi-objective topology optimization is widely adopted to address structural design problems under coupled multi-performance constraints. Never–theless, inherent flaws in weight assignment have long limited the comprehensive performance of optimized configurations. Single subjective weighting methods suffer from strong empirical interference, while purely objective weighting approaches deviate from practical engineering conditions. Neither category can effectively balance conflicting indicators including static structural stiffness and multi-order natural frequencies.

Marinković et al.[1], Farah et al.[2] and Jerman et al.[3] optimized different shell structures for lightweight and static performance, yet all adopted single-objective schemes with stress, frequency and buckling only as inequality constraints or trial-and-error geometric ad–justments. None constructed a static-dynamic coupled multi-objective model or a quantifiable weighting mec–hanism integrating engineering experience and simula–tion data, failing to balance conflicting indicators of mass reduction, stiffness and multi-order natural frequ–encies. Huang et al. [4] built a compromise program–ming multi-objective model for gearbox casing, but the weight of each objective was determined only by engineering experience, lacking objective entropy infor–mation correction.Zhang and Li[5] proposed equivalent static load conversion for dynamic topology optimi–zation, but did not construct **a** multi-objective weighting framework to coordinate stiffness, mass and natural frequencies. Barreiro et al.[6] carried out SIMP topo–logy optimization for cast gearbox housings and dis–cussed additive manufacturing feasibility, yet only took structural mass as the single objective without balancing static stiffness and multi-order vibration frequencies.

In current research on static and dynamic charac–teristic analysis and structural topology optimization of hovercraft reducer housings, scholars worldwide have conducted in-depth investigations into key issues such as structural redundancy, low material utilization, and the difficulty of synergistically optimizing lightweig–hting and dynamic performance. Studies have shown that topology optimization has become a core approach to resolving these contradictions. For example,Qi et al. [7] optimized gearbox casing for vibration and noise reduction via topology iteration, but the weight of each optimization target was assigned artificially without objective data correction from entropy theory.Townsend et al. [8] proposed level set topology optimization for stress limitation, while the trade-off between stiffness, mass and dynamic performance was not quantitatively

Received: July 2026, Accepted: August 2026
Correspondence to: Prof. Xing Cheng
Coll Intelligent Mfg Engn, China
Chongqing Univ Arts & Sci, Yongchuan, China
E-mail: bit_cx@163.com
doi: 10.5937/fme2604621C
© Faculty of Mechanical Engineering, Belgrade. Allrights reserved

weighted.Wu et al. [9] adopted cooperative-game combination weighting to fuse AHP subjective weights and entropy objective weights for multi-index evaluation, yet the weighting strategy was only applied to system capability assessment rather than structural multi-objective topology optimization.

Therefore, this paper proposes a universal multi-objective topology optimization method integrating game-theory combined weighting and compromise programming, which combines the advantages of subjective and objective weighting to coordinate multiple conflicting objectives. Using a hovercraft reducer housing as an illustrative case study, finite element simulations, optimization iterations, and structural reconstructions demonstrate that the proposed framework delivers superior convergence stability and a highly balanced multi-performance response compared with traditional single weighting strategies.

2. ESTABLISHMENT OF THE REFINED REDUCER HOUSING MODEL

2.1 Refined Model of the Housing

The reducer consists mainly of a housing structure and a transmission mechanism, with overall housing dimensions of 1350 mm × 485 mm × 1435 mm. Its internal transmission chain comprises four-stage gear transmission, sequentially arranged as an input end, reversing transmission end, intermediate transition end, and final output end.

The main reducer housing body consists of an upper housing and a lower housing. When constructing its high-fidelity refined numerical model in the finite element software ABAQUS, minor geometric simplifications were applied to secondary features such as bolt connection holes, micro chamfers, local bosses, and internal gear rings to optimize mesh topology quality while ensuring convergence efficiency. Meanwhile, local mesh refinement was performed on the main load-bearing and critical load-bearing regions of the housing. After discretization, the final numerical model contains 181,371 nodes, consisting of 12,603 hexahedral elements and 682,891 tetrahedral elements. The model uses aluminum alloy, with the following mechanical properties: elastic modulus of 68,900 MPa, density of 2.7×10□□ t/mm³, Poisson's ratio of 0.33, and yield strength of 310 MPa.

2.2 Finite Element Simulation of the Model

Calculating the loads on the housing is the prerequisite for static simulation [10]. External loads on the housing mainly originate from the meshing interaction of gear pairs at each stage. Specifically, the tangential force F_t, radial force F_r, and axial force F_a generated by gear transmission first act on the shafting, then transfer to the bearing support boundaries, and are finally applied to the reducer housing as concentrated or distributed loads. The force application positions on the housing are shown in Figure 1 and Table1.

Since loads are applied to each shaft, eight reference points RP1–RP8 were defined in ABAQUS to couple with the corresponding bearings. Applying loads to these points can replace direct loading on the bearings [11].

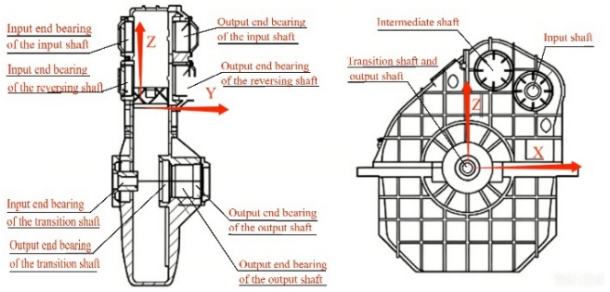


Figure 1. Force diagram of the housing

Table 1. Forces at the bearing seats of the housing

Bearing seat	F_x (kN)	F_y (kN)	F_z (kN)
Input end bearing of the input shaft	-5.6	-11.0	0
Outputend bearing of the input shaft	1.6	-34.8	-11.5
Input end bearing of the reversing shaft	-27.0	30.6	0
Output end bearing of the reversing shaft	-4.4	42.0	3.7
Input end bearing of the transition shaft	12.6	-29.3	7.8
Output end bearing of the transition shaft	23.4	-2.6	0
Input end bearing of the output shaft	0	0.1	0
Output end bearing of the output shaft	0	-0.5	0

Meanwhile, the upper and lower housings were connected via a tie constraint, with the upper housing connection surface as the master surface and the lower housing connection surface as the slave surface. The boundary condition was set as the outer surface of the output shaft output end being fully fixed.

2.3 Static Characteristics of the Model

Static analysis was performed on the reducer housing, and stress and displacement contours were extracted. The results are shown in Figure 2 and Figure 3.

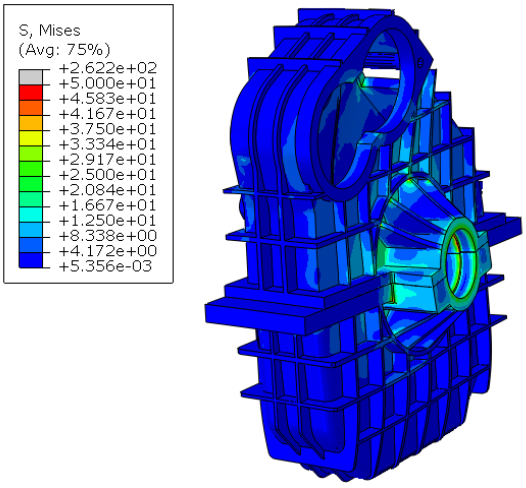


Figure 2. Stress contour of the housing

The maximum stress of the housing is 262 MPa, occurring above the stiffening rib at the output shaft output end. Stress is mainly concentrated at the output shaft output end and the transition shaft input end, while equivalent stress at other positions is relatively low.

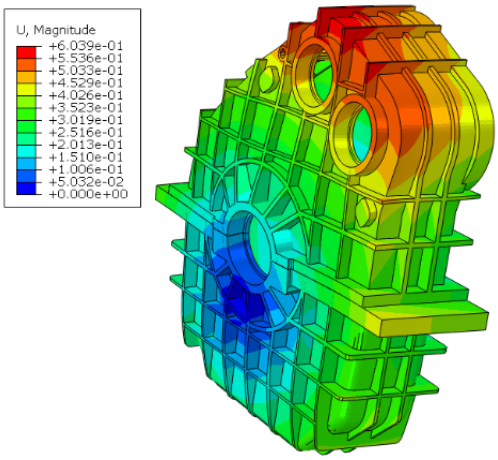


Figure 3. Displacement contour of the housing

The maximum displacement of the housing is 0.6039 mm, occurring above the bearings at the input shaft input end and reversing shaft input end on the upper housing. Displacement decreases gradually from top to bottom.

The safety factor of the housing under working conditions is 310/262=1.18,so ensuring housing stiff–ness is critical.

2.4 Modal Analysis

To suppress dynamic vibration and minimize acoustic radiation under operational excitations, the constrained modal characteristics of the initial housing were eva–luated (Figures 4–7).

The hovercraft reducer is subject to extremely complex excitations during operation. A frequency of 200 Hz typically corresponds to the rotational funda–mental frequency of high-power engines, high-order nonlinear shaft vibration, or the meshing frequency of gear pairs at specific speeds. The fourth-order natural frequency (203.8 Hz) poses a potential resonance risk due to its proximity to the dominant 200 Hz operational excitation frequency. Conversely, the first three modes correspond to localized deformations that exert negli–gible impact on global structural stability.

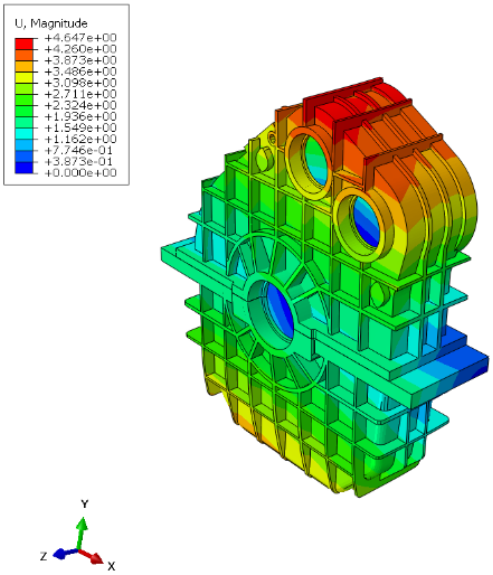


Figure 4. First-order mode shape

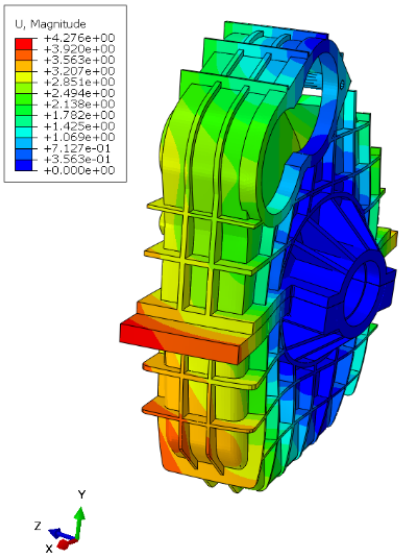


Figure 5. Second-order mode shape

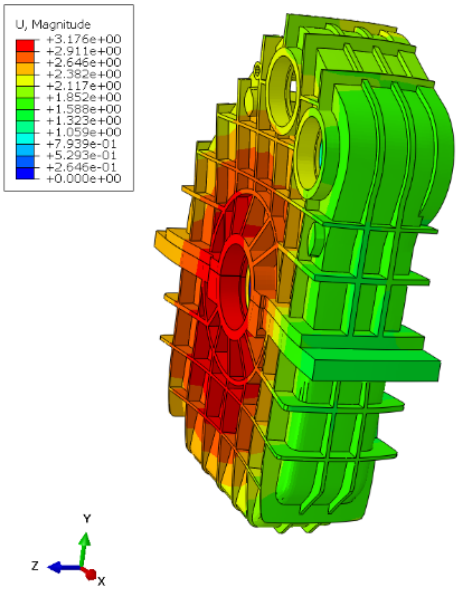


Figure 6. Third-order mode shape

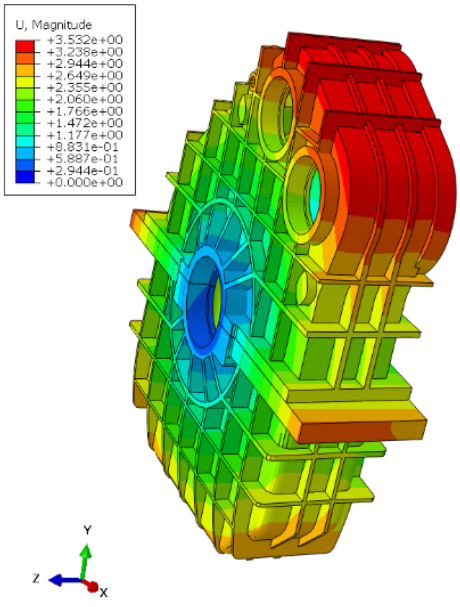


Figure 7. Fourth-order mode shape

Table 2. Natural frequencies and mode shapes of the housing

Order	Natural frequency (HZ)	Maximum deformation region	Mode shape description
1	91.8	Top structure	First-order fundamental bending
2	114.0	Unilateral horizontal flange	First-order axial torsion
3	153.6	Left middle annular panel	Local breathing / panel bulging
4	203.8	Top structure and both bottom sides	High-order combined bending / shear

3. GAME-THEORY BASED AHP-ENTROPY COMBINED WEIGHTING METHOD

Index weighting methods are generally divided into subjective and objective categories. The Analytic Hie–rarchy Process (AHP) is a classic subjective weighting method with high uncertainty and low result credibility. The entropy weight method is a classic objective weighting method, but it relies heavily on original data and may deviate from practical engineering by ignoring subjective experience. To overcome the limitations of both methods, a combined weighting method based on game theory is proposed to integrate their advantages and determine the weights of five optimization indi–cators [12].

The core of AHP is to numerically map the relative importance of evaluation indicators. In practice, desig–ners assign discrete scores on a 1–9 scale based on the relative importance of factors, or use even intermediate values according to engineering conditions, to construct a judgment matrix.

$$A = a_{ij} = \begin{pmatrix} a_{11} & a_{12} & \cdots & a_{1n} \\ a_{21} & a_{22} & & a_{2n} \\ \vdots & & \ddots & \vdots \\ a_{n1} & a_{n2} & \cdots & a_{nn} \end{pmatrix} \quad (1)$$

where n is the total number of indicators; a_{ij} is the relative importance of indicator a_i to indicator a_j, i.e.,aij = a_i/a_j (i,j=1,2,…,5). Based on simulation results of st–ructural static and dynamic characteristics, this study selected five core parameters — deformation stiffness and the first four natural frequencies — as evaluation indicators for topology optimization. The pairwise comparisons in the AHP model were formulated based on baseline stress-strain responses. Given that the initial peak displacement (1.449 mm) compromises gear meshing fidelity and the peak stress approaches the yield strength (310 MPa), static compliance mini–mization was assigned higher priority relative to modal frequencies. In terms of dynamics, the first-order natural frequency involves global structural bending and is most likely to induce overall resonance, so it has the highest weight. The second-order frequency involves local side flange torsion, with secondary importance. The third and fourth orders are high-frequency local modes with less impact on global structural stability, so their importance decreases sequentially. The resulting comparison matrix is:

$$A = a_{ij} = \begin{pmatrix} 1 & 3 & 4 & 5 & 6 \\ 1/3 & 1 & 2 & 3 & 4 \\ 1/4 & 1/2 & 1 & 2 & 3 \\ 1/5 & 1/3 & /12 & 1 & 2 \\ 1/6 & 1/4 & 1/3 & 1/2 & 1 \end{pmatrix} \quad (2)$$

After consistency check and normalization, the results are as follows:

$$C_{\mathrm{CR}} = \frac{C_{\mathrm{CI}}}{R_{\mathrm{RI}}} = \frac{\lambda - m}{(m-1)R_{\mathrm{RI}}} = 0.0152 < 1 \quad (3)$$

where C_{CI} is the consistency index of the judgment matrix; λ is the maximum eigenvalue of the matrix; m is the order of the matrix; and the random consistency index RRI is 1.12 for this case. After passing the consistency test, the principal eigenvector of judgment matrix A (the normalized vector corresponding to the maximum eigenvalue) was calculated, and the final weights of the five core indicators were obtained:

$$C_1 = (\ 0.4174, 0.2634, 0.1602, 0.0975, 0.0615\ )$$

The entropy weight method is a classic objective weighting method. Its core idea is to use information entropy to measure the data dispersion of each indicator. An indicator with larger data variation and higher dispersion during iteration contains more information and is more sensitive to optimization results, so it is assigned a higher weight.

Consider a decision problem with m schemes and n evaluation indicators, with the original decision matrix $\mathbf{X} = [x_{ij}]_{m\times n}$. To unify indicator trends, cost-type indi–cators (smaller-is-better) are first positively normalized, typically via reciprocal or difference transformation. In this study, reciprocal transformation is applied to comp–liance C:

$$x_{i1} = \frac{1}{C_i}, i = 1, 2, ..., m \quad (4)$$

Frequency indicators (larger-is-better) retain their original values, i.e., $x'_{ij} = f_{i,j\text{-}1}$ (j = 2, …,5) The norma–lized matrix is denoted $\mathbf{X}' = [x'_{ij}]$m×n, hereinafter refe–rred to as x_{ij}. The proportion matrix is then calculated: for each indicator j, the proportion p_{ij} of the i-th scheme is:

$$p_{ij} = \frac{x_{ij}}{\sum_{i=1}^{m} x_{ij}}, i = 1, ..., m;\ j = 1, ..., n \quad (5)$$

This yields the probability matrix $\mathbf{P} = [p_{ij}]$.

Next, the information entropy is calculated. The information entropy e_j of the j-th indicator is defined as:

$$e_j = -k\sum_{i=1}^{m} p_{ij} \ln\left(p_{ij}\right), j = 1, ..., n \quad (6)$$

where the constantk k = 1/ln(m), to ensure $0 \le e_j \le 1$. When $p_{ij} = 0$, $p_{ij}\ln(p_{ij}) = 0$ by definition.

The difference coefficient and objective weights are then calculated. The difference coefficient g_j reflects the

data dispersion of indicator j:

$$g_j = 1 - e_j \tag{7}$$

A larger g_j indicates more information provided by the indicator and a higher corresponding weight. Normalizing the difference coefficients gives the objective weights of each indicator:

$$w_j^{\text{obj}} = \frac{g_j}{\sum_{j=1}^{n} g_j}, \text{ satisfying } \sum_{j=1}^{n} w_j^{\text{obj}} = 1 \tag{8}$$

To balance decision-maker experience and inherent data patterns, the combined weighting method integrates the objective weights w_j^{obj} from the entropy weight method and the subjective weights w_j^{sub} from AHP. The multiplicative synthesis method is adopted:

$$w_j^{\text{comb}} = \frac{w_j^{\text{sub}} \cdot w_j^{\text{obj}}}{\sum_{j=1}^{n} \left(w_j^{\text{sub}} \cdot w_j^{\text{obj}} \right)} \tag{9}$$

4. GENERAL MULTI-OBJECTIVE TOPOLOGY OPTIMIZATION MODEL BASED ON COMPROMISE PROGRAMMING

4.1 Construction of the Multi-Objective Topology Optimization Function

The multi-objective topology optimization mathematical model established in this section is universal for all transmission housings, and the hovercraft gearbox is only used to solve and verify the model.

For static stiffness problems, the topology objective of maximizing structural stiffness is usually equivalently transformed into minimizing structural global compliance to facilitate mathematical solution. In multi-objective topology optimization, the compromise programming method is a classic standardized solution approach. Its core idea is to find a topology solution that minimizes the geometric distance between the actual values of each sub-objective (compliance, natural frequencies) and their respective ideal solutions.

Let the topology optimization variable (e.g., element density in the variable density method) be x, and the five sub-objective functions be $f_1(x)$, $f_2(x)$, $f_3(x)$, $f_4(x)$, $f_5(x)$, corresponding to minimizing compliance and maximizing the 1st to 4th natural frequencies, respectively. Before optimization, five single-objective topology optimizations are typically performed, or the ideal solution (f^*_i) and nadir solution (f^{ns}_i) of each indicator are determined empirically. For compliance $f_1(x)$, f^*_i is the minimum compliance from single-objective optimization, and f^{ns}_i is the maximum compliance. For natural frequencies $f_i(x)$ = (i=2,3,4,5), f^*_i is the maximum achievable value of that order, and f^{ns}_i is the minimum value.

Sub-objective normalization is then performed. Since compliance and natural frequency differ in magnitude and unit, dimensional effects must be eliminated, and all objectives are uniformly converted to minimization form (0 = ideal, 1 = worst). Compliance (minimization objective) is normalized as:

$$F_1(x) = \frac{f_1(x) - f_1^*}{f_1^{ns} - f_1^*} \tag{10}$$

Natural frequencies (maximization objectives) are normalized as:

$$F_i(x) = \frac{f_1^* - f_i(x)}{f_i^* - f_1^{ns}} (i = 2,3,4,5) \tag{11}$$

All $F_i(x)$ values are thus bounded within the interval [0,1].

The comprehensive objective function for multi-objective topology optimization is derived via the compromise programming method:

$$\min F(x) = \left| \sum_{i=1}^{5} w_i \cdot \left(F_i(x) \right)^p \right|^{\frac{1}{p}} \tag{12}$$

In this study, p=2, representing the shortest Euclidean distance from the current topology solution to the absolute ideal point in multidimensional space. This avoids extreme solutions where one objective performs poorly while others perform well, and drives the topology result toward balanced performance across all indicators. Expanding the formula gives:

$$\begin{aligned} \min F(x) = \Big\{ & w_1 \cdot \left(F_1(x) \right)^2 + w_2 \cdot \left(F_2(x) \right)^2 + \\ & + w_3 \cdot \left(F_3(x) \right)^2 + w_4 \cdot \left(F_4(x) \right)^2 + w_5 \cdot \left(F_5(x) \right)^2 \Big\}^{\frac{1}{2}} \end{aligned} \tag{13}$$

where w_1, w_2, w_3, w_4, w_5 are the weights corresponding to compliance and the 1st to 4th natural frequencies, respectively.

Topology optimization was performed using the optimization module of ABAQUS, which adopts the variable density method. The basic idea of the variable density method is to introduce hypothetical material elements with continuously variable density. However, this leads to numerous intermediate-density elements in optimization results, reducing manufacturability. The Solid Isotropic Material with Penalization (SIMP) interpolation model introduces a penalty factor q to suppress intermediate-density elements, accelerating the convergence of element densities toward 0 and 1 [13]. The objective function is set as the comprehensive function $F(x)$, with volume fraction V^a as the constraint. The mathematical model is:

$$\begin{aligned} & \min F(x) \\ s.t. & \begin{cases} V \le V^a \\ 0 < \rho_{\min} < \rho_i \le 1 \\ E = \rho_i^q \left(E_0 - E_{\min} \right) T \end{cases} \end{aligned} \tag{14}$$

where V is the housing volume fraction, V^a = 0.7; ρ is element density, and ρ_i is the density of the i-th element; E_0 is the initial elastic modulus, and E is the optimized elastic modulus; q is the penalty factor, set to 3.

4.2 Implementation of Multi-Objective Topology Optimization

Structural topology optimization seeks the optimal distribution of limited material within a specified design domain under given load and support constraints to meet prescribed performance requirements [14].

Topology optimization can generate conceptual design schemes in the early design phase and determine the optimal structural layout. It breaks the traditional iterative "design–verification–revision" cycle, improving design efficiency and quality while shortening development cycles and reducing costs. The finite element model for topology optimization is shown below. Static simulation confirms that the reducer housing has significant topology reshaping potential. In this study, critical load-bearing features such as bolt holes and bearing seats on the upper and lower housings are designated as non-design domains, while the remaining housing area is designated as the topology design domain. Figure 8 shows the finite element model, and Figure 9 shows the optimization flow.

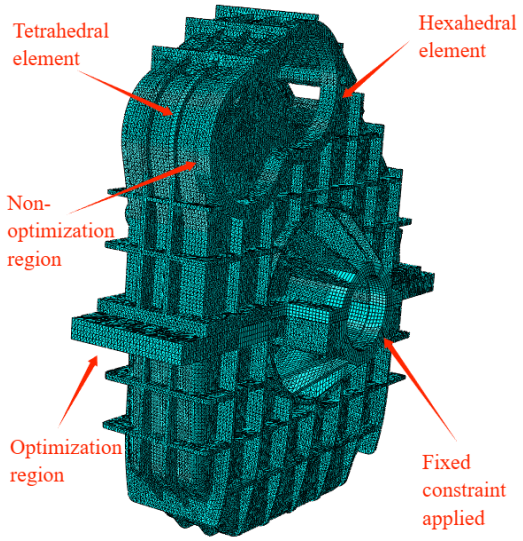


Figure 8. Finite element model diagram

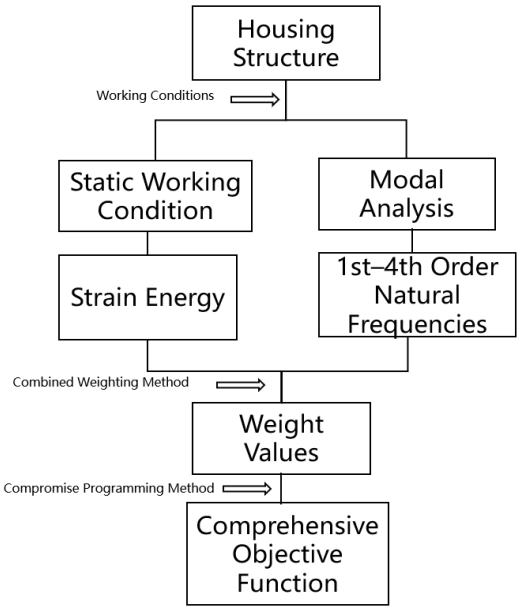


Figure 9. Optimization flow chart

As shown in Equation (13), the extreme values of the five sub-objectives are required for dimensional normalization before multi-objective topology optimization. Therefore, single-objective topology optimizations were first performed for each sub-objective[12]. Single-objective optimizations were conducted in ABAQUS with minimum compliance and maximum first four natural frequencies as objectives, and volume fraction as the constraint. The extreme values of each sub-objective were extracted from the results and substituted into the formula, with the comprehensive function $F(x)$ as the optimization objective and volume fraction as the constraint.

Figures 10–14 show the single-objective optimization results, with compliance, 1st to 4th natural frequency as the respective objectives, and volume fraction $\leq 70\%$ of the initial value as the constraint.

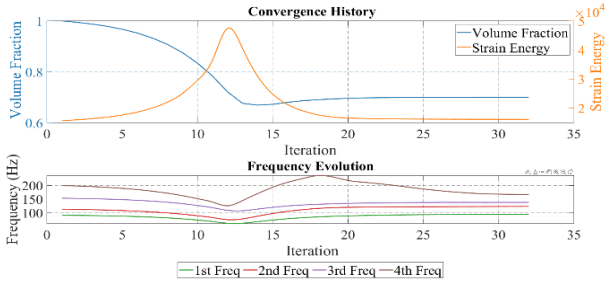


Figure 10. Iteration process with compliance as the optimization objective

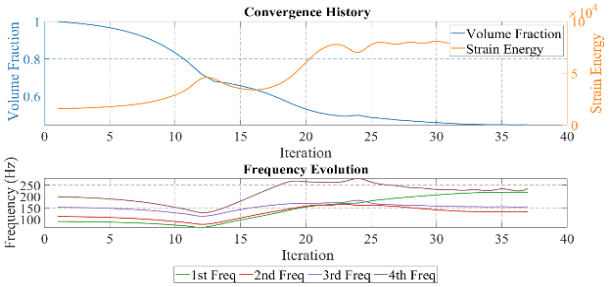


Figure 11. Iteration process with the first-order frequency as the optimization objective

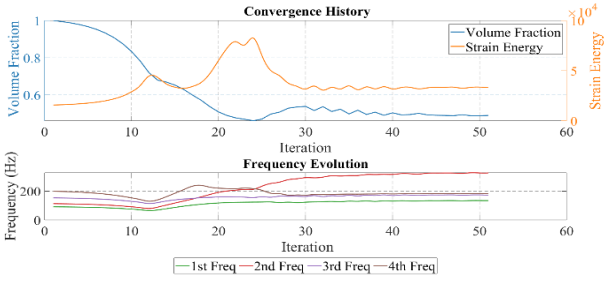


Figure 12. Iteration process with the second-order frequency as the optimization objective

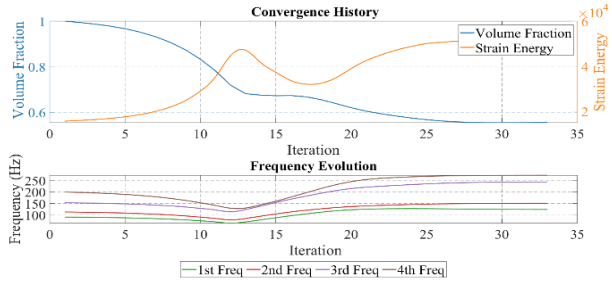


Figure 13. Iteration process with the third-order frequency as the optimization objective

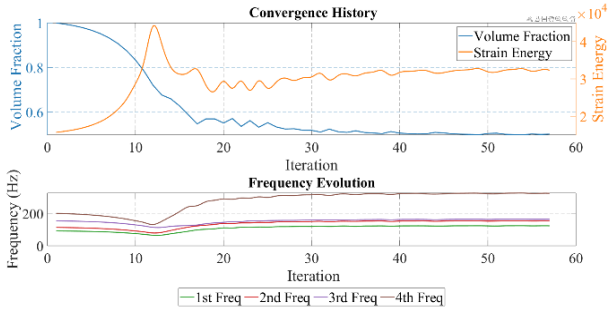


Figure 14. Iteration process with the fourth-order frequency as the optimization objective

Table 3. Single-objective optimization results

Optimization objective	Compliance	1st-order frequency	2nd-order frequency	3rd-order frequency	4th-order frequency
Compliance	16129.9	94.4	123.5	138.2	167.0
1st-order frequency	72814.7	218.6	133.5	155.9	236.1
2nd-order frequency	33148.9	134.6	326.8	172.8	182.6
3rd-order frequency	51010.7	124.3	151.0	243.6	272.3
4th-order frequency	32286.6	123.0	153.2	162.9	323.1

Table 4. Results of the entropy weight method

Optimization sub-objective	Information entropy	Difference coefficient	Objective weight	Weight percentage
Compliance	0.9186	0.0814	0.4337	43.37%
1st-order frequency	0.9735	0.0265	0.1412	14.12%
2nd-order frequency	0.9515	0.0485	0.2584	25.84%
3rd-order frequency	0.9873	0.0127	0.0677	6.67%
4th-order frequency	0.9814	0.0186	0.0990	9.90%

The weight vector of the five indicators is C_2 = (0.4337,0.1412,0.2584,0.0677,0.0990)

Table 5. Weights from three weighting methods

Optimization sub-objective	AHP subjective weight	Entropy objective weight	Combined weight
Compliance	0.4174	0.4337	0.6649
1st-order frequency	0.2634	0.1412	0.1366
2nd-order frequency	0.1602	0.2584	0.1520
3rd-order frequency	0.0975	0.0677	0.0242
4th-order frequency	0.0615	0.0990	0.0223

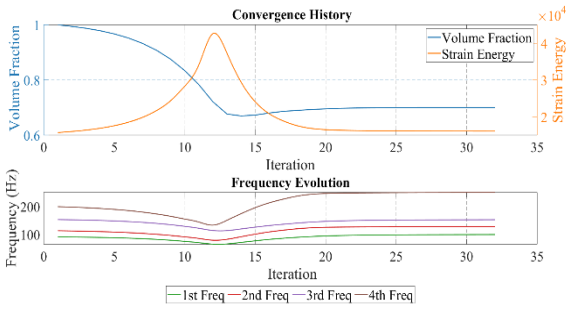


Figure 15. Iteration process with AHP subjective weights

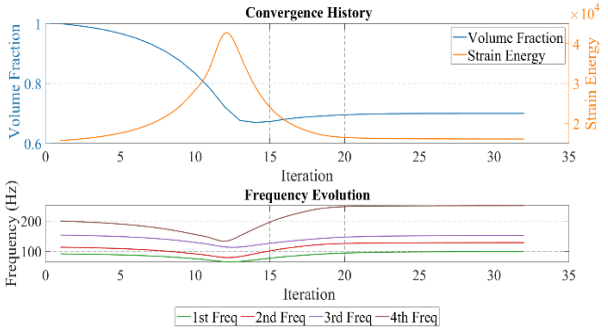


Figure 16. Iteration process with entropy weight objective weights

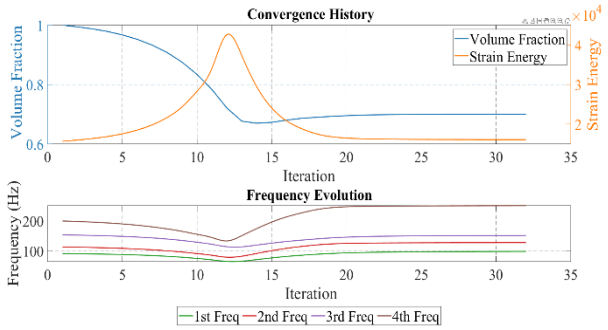


Figure 17. Iteration process with combined weights

Table 6. Optimization results of three weighting methods

Method	Compliance	1st-order frequency	2nd-order frequency	3rd-order frequency	4th-order frequency
AHP	16077.6	99.7	128.5	152.9	251.1
Entropy weight method	16078.0	99.3	128.6	152.4	251.0
Combined weighting method	16078.6	98.7	127.9	151.4	250.7

Figures 15–17 present the results of the three methods. The limitation of AHP subjective weights is that they rely purely on expert experience and subjective preference. While they can reflect engineering priorities for specific frequencies or stiffness, they tend to ignore inherent data fluctuations and sensitivity information. The limitation of entropy weight objective weights is that weights are assigned purely based on data infor–mation entropy. Although they eliminate subjectivity, they are susceptible to interference from local numerical fluctuations (e.g., sudden compliance increases during transition phases) and lack clear engineering physical guidance.

Regarding compliance convergence, the combined weighting method demonstrates heightened sensitivity to design variable gradients, fostering an efficient material redistribution under volume constraints. Cru–cially, it enhances global search capability, allowing the solver to bypass local optima during rapid stiffness transitions, resulting in a more robust convergence path.

After 31 iterations, the multi-objective optimized structure was obtained, as shown in Figure 18. The raw topology result contains numerous triangular and fragmented structures that do not meet manufacturing requirements, so model reconstruction is necessary.

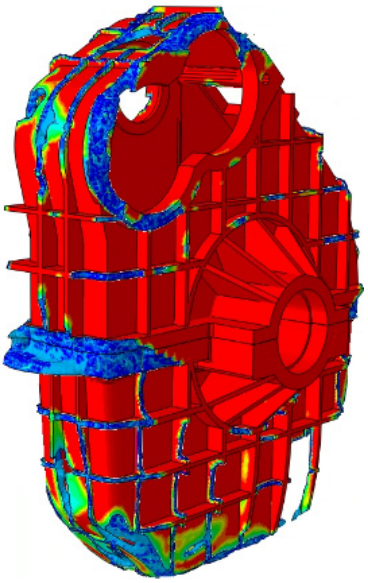


Figure 18. Topology optimized structure diagram

5. MODEL RECONSTRUCTION AND RESULT COMPARISON

5.1 Model Reconstruction

This chapter takes a hovercraft reducer gearbox as a typical engineering example to verify the performance of the general game-theory combined weighting multi-objective topology optimization framework proposed in Chapter 3 and Chapter 4.

To verify the rationality and accuracy of the topology optimization results, secondary redesign of the reducer housing was performed. Based on the material distribution indicated by the topology density map, a local stiffening rib scheme was designed: redundant material and conservative configurations were removed, and targeted reinforcement was applied to weak load-bearing regions.

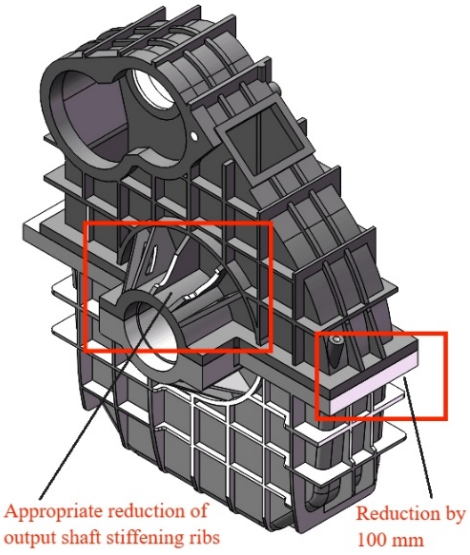


Figure 19. Model modification diagram (1)

Static analysis results show that stress is mainly concentrated at the junctions between stiffening ribs and the housing, while the lower housing stiffening ribs bear relatively low loads. Topology optimization results show low material density in the lower housing stiffening ribs, so this optimization focuses mainly on the lower housing stiffening ribs. The specific modification positions are shown in Figures 19 and 20.

With aluminum alloy material parameters, the housing mass before and after optimization was compared. The results show that the housing mass decreases from 256 kg to 245 kg, with a total weight reduction of 11 kg, corresponding to a 4.2% weight reduction rate.

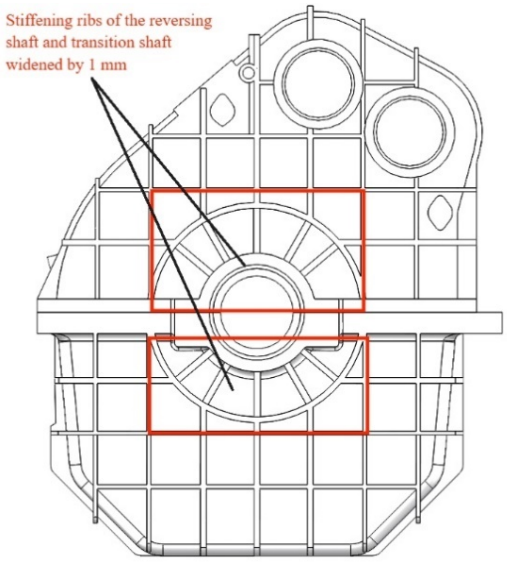


Figure 20. Model modification diagram (2)

5.2 Comparative Analysis Before and After Optimization

Strength analysis of the optimized housing yields the following results:

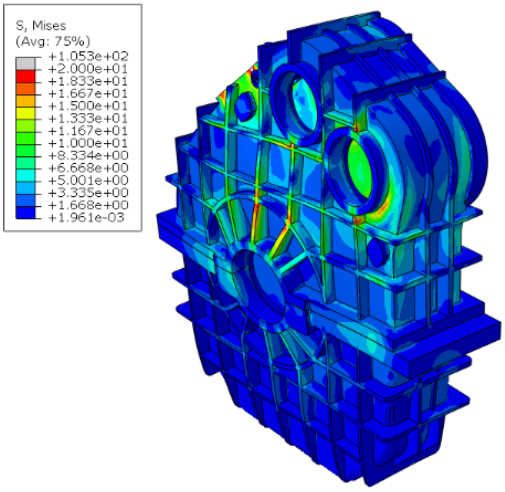


Figure 21. Stress contour of the optimized housing (1)

As shown in Figures 21–24, after optimization, the maximum stress of the housing is approximately 105.3 MPa, occurring at the junction between stiffening ribs and the housing, with stress overall concentrated in the upper housing.

The maximum displacement is approximately 0.6985 mm, located above the bearings at the input shaft input end and reversing shaft input end on the upper housing. Displacement decreases gradually from top to bottom, and is zero at the fixed bearing positions.

Modal analysis of the optimized housing is shown in Figures 25–28:

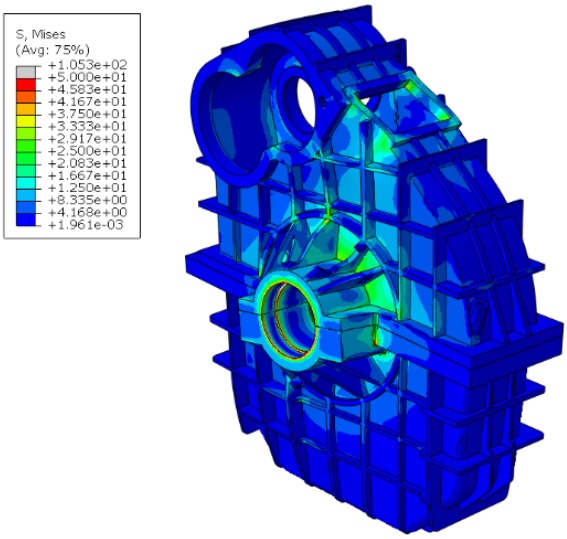


Figure 22. Stress contour of the optimized housing (2)

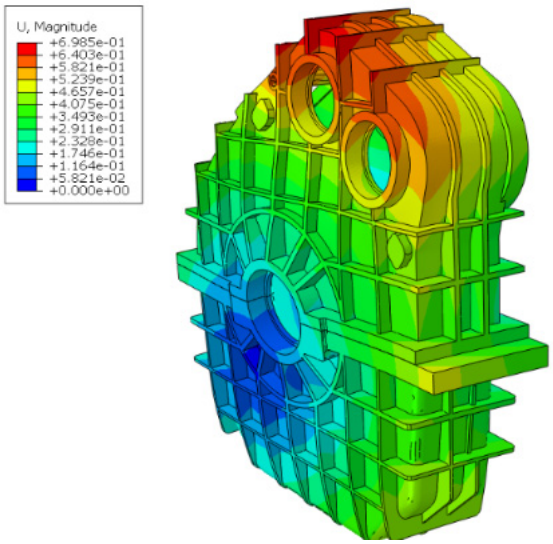


Figure 23. Displacement contour of the optimized housing (1)

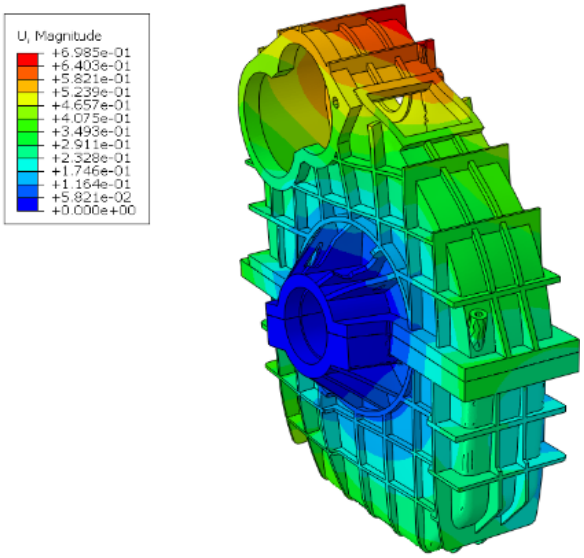


Figure 24. Displacement contour of the optimized housing (2)

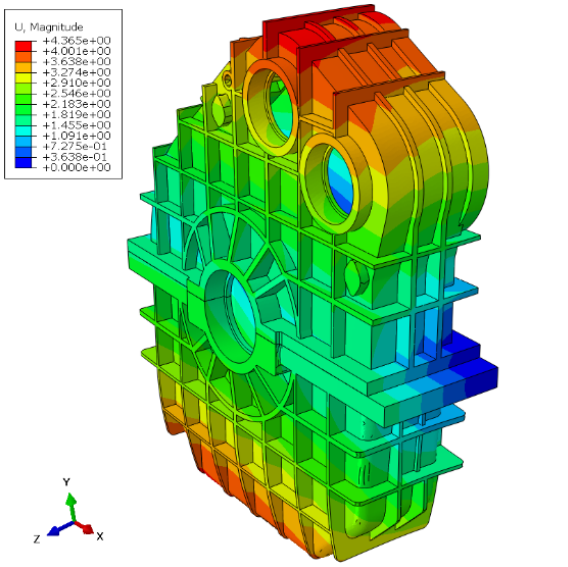


Figure 25. First-order mode shape of the optimized housing

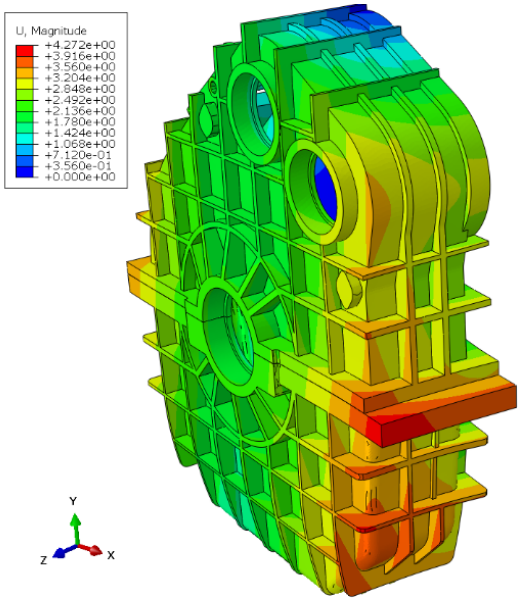


Figure 26. Second-order mode shape of the optimized housing

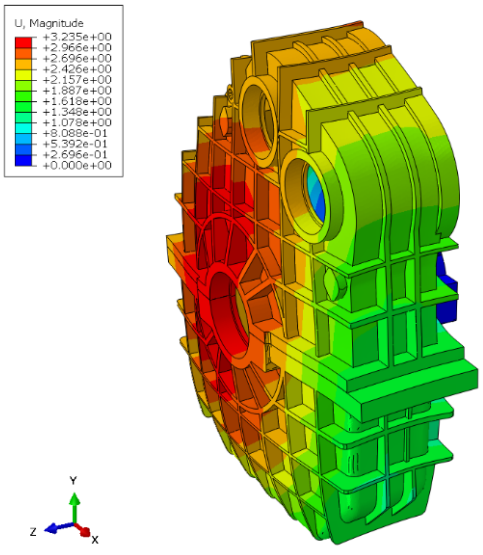


Figure 27. Third-order mode shape of the optimized housing

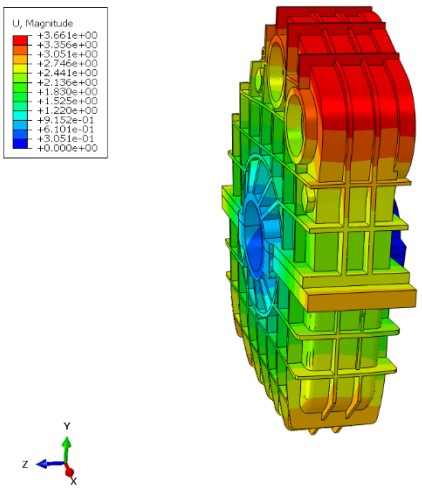


Figure 28. Fourth-order mode shape of the optimized housing

Table 7. Natural frequencies and mode shapes of the optimized housing

Order	Natural frequency (Hz)	Maximum deformation region
1	73.9	Top structure and bottom region
2	107.0	Near the bottom of the housing joint
3	134.8	Near the transition shaft input end bearing
4	208.2	Top structure

Comparing the results before and after optimization yields the following findings:

Table 8. Performance comparison before and after optimization

Indicator	Before optimization	After optimization	Change rate
Mass (kg)	256	245	4.2%
Stress(MPa)	262	105.3	60.0%
Displacement (mm)	0.6039	0.6985	-15.6%
1st-order frequency (Hz)	91.8	73.9	19.4%
2nd-order frequency(Hz)	114.0	107.0	6.1%
3rd-order frequency(Hz)	153.6	134.8	12.2%
4th-order frequency(Hz)	203.8	208.2	-2.1%

This study aims to reduce structural mass, maximize static stiffness, and increase the first four natural frequencies. Model reconstruction and secondary simulation verification were performed on the hovercraft reducer housing using different sub-objective weighting strategies. Comparative evaluation yields key structural insights:

1. Housing mass is reduced by 4.2%, maximum stress is reduced by 60.0%, and maximum displacement increases by 15.6%.In terms of static strength, under the constraint of minimal overall geometric modification, the primary stress transmission paths are altered to achieve substantial stress relief at the cost of a marginal displacement increment, thereby enhancing structural reliability.

2. The first three natural frequencies decrease: the first-order frequency decreases by 19.4%, the second-order by 6.1%, and the third-order by 12.2%. The fourth-order frequency increases by 2.1%, which to some extent avoids the 200 Hz excitation frequency and significantly improves the vibration resistance and acoustic performance of the reducer housing.

3. The combined weighting strategy integrates the advantages of AHP and the entropy weight method, fully verifying its superiority. This method overcomes the low credibility of subjective weighting and addresses the problem that objective weighting is overly dependent on sample data and may deviate from engineering practice. It provides a theoretical basis for multi-objective topology optimization research on hovercraft reducer housings.

6. CONCLUSION

To resolve the subjectivity-objectivity imbalance in conventional multi-objective topology optimization, a universal framework integrating game-theory combined weighting with compromise programming was established to balance static strength and dynamic performance. Simulation analysis is carried out with the hovercraft reducer housing as an engineering example, and the conclusions are drawn as follows:

1. Compared with the single AHP weighting scheme and single entropy-weight scheme, the game-theory-based combined weighting strategy exhibits more stable iterative convergence performance and can balance multiple conflicting static and dynamic optimization objectives.

2. The topological configuration obtained by the proposed method realizes structural lightweight design. The optimized structure effectively avoids excitation frequencies to reduce resonance risk, while the stress level is improved simultaneously.

3. The proposed optimization framework is not limited to hovercraft reducer housings. It can be extended to the static-dynamic collaborative lightweight design of various transmission housings, which provides a feasible technical approach for multi-objective topology optimization of mechanical structures.

REFERENCES

[1] Marinković, A.: Structural Optimisation of Planetary Gearbox Components, FME Transactions, 53, pp. 74-84, 2025.

[2] Farah, S., Khalfallah, S.: A Design Optimization Strategy of an Aircraft Composite Wing-Box Based on a Multi-scale FEA, FME Transactions, 53, pp. 187-198, 2025.

[3] Jerman, B.: Optimization of the support structure of large axial-radial bearing of overhead type manipulator, FME Transactions, 46, pp. 386-391, 2018.

[4] Huang, H., Wang, Z.: Multi-objective topology optimization of aero-engine accessory gearbox case based on compromise programming method, Science China Technological Sciences, 68, pp. 223-237, 2025. (in Chinese)

[5] Zhang, L., Li, Y.: A Fail-Safe Topology Optimi–zation Method for Structures Under Dynamic Loads, Journal of Applied Mechanics, 92, pp. 1-12, 2025.

[6] Barreiro, P., Bronner, A., Hoffmeister, J.: New improvement opportunities through applying topo–logy optimization combined with 3D printing to the construction of gearbox housings, Forschung im Ingenieurwesen, 83, pp. 669-681, 2019.

[7] Qi, L., Zhou, J.X., Jin, P.C.: Low noise optimi–zation of two-stage gearbox housing structure based on acoustic contribution analysis and topology optimization, Journal of Mechanical Science and Technology, 37, pp. 4533-4544, 2023.

[8] Townsend, S., Brampton, C.: Stress-based shape and topology optimization with the level set method, Computer Methods in Applied Mechanics and Engineering, 329, pp. 1-23, 2018.

[9] Wu, C., Wang, Y., Gao, S.: Service capability evaluation of electric vehicle charging and battery swapping stations as a function of a game theory based combination weighting method, IET Energy Systems Integration, 6, 4, pp. 581-592, 2024.

[10] Zhang, Y.A. et al.: Multi-objective optimization of high-power tractor gearbox housing based on improved NSGA-□, Transactions of the Chinese Society for Agricultural Machinery, 53, pp. 310-319, 2022. (in Chinese)

[11] Song, S.F. et al.: Finite element analysis on static strength of a diesel engine block, Internal Combus–tion Engine & Powerplant, 35, pp. 47-51, 2018. (in Chinese)

[12] Liu, W. et al.: Static and dynamic characteristic analysis and multi-objective topology optimization of gear housing, Journal of Mechanical Strength, 47, pp. 94-102, 2025. (in Chinese)

[13] Wu, D.F. Research on continuum structure topo–logy optimization based on variable density met–hod, Xidian University, 2010. (in Chinese)

[14] Wei, J., Li, Z., Sun, W., et al.: Structure optimi–zation of high-speed EMU gearbox based on SIMP and compliance theory, Journal of Mechanical Strength, 33, pp. 558-564, 2011. (in Chinese)

Acronyms and abbreviations

AHP	Analytic Hierarchy Process
CAD	Computer Aided Design
FEA	Finite Element Analysis
SIMP	Solid Isotropic Material with Penalization

NOMENCLATURE

F_t	Tangential Force
F_r	Radial Force
F_a	Axial Force
F_x	Force in the x-axis direction
F_y	Force in the y-axis direction
F_z	Force in the z-axis direction
RP1-8	Reference points coupling bearing seats
a_{ij}	pairwise comparison matrix
CCR	consistency deviation measurement
	maximum eigenvalue
λ	unique non-zero eigenvalue
m	consistency test parameter
p_{ij}	probability matrix
e_i	information entropy
g_i	difference coefficient
w_j^{obj}	objective weights
w_j^{sub}	subjective weights
$f_n(x)$	sub-objective function
C_1,C_2	weight values

ИНТЕГРИСАНИ ОКВИР ЗА ВИШЕ–КРИТЕРИЈУМСКУ ТОПОЛОШКУ ОПТИМИ–ЗАЦИЈУ ЗАСНОВАН НА КОМБИНОВАНОМ ОДРЕЂИВАЊУ ТЕЖИНСКИХ КОЕФИЦИЈЕНАТА: МЕТОДОЛОГИЈА И ПРИМЕНА НА РЕДУКТОР ХОВЕРКРАФТА

К. Шенг, Ш. Жоу, К. Ли, Т. Ли, Ф. Жанг, К. Пенг, Х. Сонг

У циљу превазилажења ограничења која прате методе са појединачним тежинским коефицијентима и компромиса између статичких и динамичких кара–ктеристика приликом тополошке оптимизације ре–дуктора, у овом раду се предлаже универзални вишекритеријумски оквир који обједињује комбиновано одређивање тежинских коефицијената на основу теорије игара (комбинација AHP методе и методе ентропије) и методу компромисног програмирања. Применом ове методе на кућиште редуктора ховеркрафта успостављен је модел за заједничку расподелу тежинских коефицијената, којим се повезују крутост (инверзна вредност деформабилности) и прве четири сопствене фреквенције. Тополошка оптимизација спроведена помоћу SIMP методе променљиве густине и накнадне CAD рекон–струкције показује супериорну робусност конвер–генције у поређењу са стратегијама које користе појединачне тежинске коефицијенте. Оптимизовано кућиште остварује смањење масе од 4,2% и смањење максималног напона од 60,0%, уз истовре–мено повећање сопствене фреквенције четвртог реда, чиме се успешно избегава опсег побуде од 200 Hz. Ова генерализована методологија пружа стандарди–зоване смернице за заједничку оптимизацију кућишта преносника према више критеријума перформанси.